The Journal of Chemical Physics

War and peace between electrostatic and van der Waals forces regulate translational and rotational diffusion

Cite as: J. Chem. Phys. **157**, 080901 (2022); https://doi.org/10.1063/5.0098506
Submitted: 09 May 2022 • Accepted: 21 July 2022 • Accepted Manuscript Online: 27 July 2022 • Published Online: 22 August 2022

Dmitry V. Matyushov

The Journal of Chemical Physics PERSPECTIVE scitation.org/journal/jcp

War and peace between electrostatic and van der Waals forces regulate translational and rotational diffusion

Cite as: J. Chem. Phys. 157, 080901 (2022); doi: 10.1063/5.0098506
Submitted: 9 May 2022 • Accepted: 21 July 2022 •
Published Online: 22 August 2022 • Corrected: 23 August 2022

Dmitry V. Matyushov[a)]

AFFILIATIONS

School of Molecular Sciences and Department of Physics, Arizona State University, P.O. Box 871504, Tempe, Arizona 85287-1504, USA

[a)]Author to whom correspondence should be addressed: dmitrym@asu.edu

ABSTRACT

In the Stokes–Einstein picture, diffusion of a Brownian particle or a molecule in a liquid solvent is caused by unbalanced fluctuations of osmotic forces on different sides of the particle. When the particle carries a charge or a higher multipolar moment, this picture is amended by fluctuations of electrostatic forces producing dielectric friction. Dielectric friction slows down both the translational and rotational diffusion. While this picture is well established and is physically sound, standard theories grossly overestimate the magnitude of dielectric friction for small dipolar solutes and larger colloidal particles, such as proteins. Motivated by recent simulation studies, this Perspective discusses the interplay between osmotic (van der Waals) and electrostatic forces in promoting molecular and colloidal diffusion. Much can be learned about microscopic friction mechanisms from statistical and dynamical correlations between osmotic and electrostatic forces.

I. INTRODUCTION

The Stokes–Einstein mechanism of diffusivity[1,2] in liquids is based on the idea that random motions of a tagged (Brownian) particle are caused by stochastic bombardment by the liquid molecules. Even though restated in many textbooks, this picture is hardly accurate when diffusion in liquids is concerned. Single-molecule collisions are not possible in dense liquids, and one has to view random walks of a tagged particle as caused by collective excitations of the liquid producing force imbalances on different sides of the particle. This is the view of diffusivity interrogated here. This Perspective aims at constructing a physical picture of how two major forces present in polar liquids, nonpolar van der Waals (vdW) and electrostatic forces, come in peace with each other to establish zero force at mechanical equilibrium, but have to compete with each other to produce random kicks responsible for translational and rotational diffusion.

The vdW interactions are universal as they act between all types of atoms of the tagged particle and the surrounding medium. They are also relatively short-ranged and induce forces and torques acting on the particle surface. Their imbalances on different sides of the particle are caused by uncompensated density fluctuations, in contrast to individual molecular collisions. This is the picture of Brownian motion originally advocated by Einstein. In his follow-up paper on Brownian motion published in 1908,[3] he noted that the physical driving force of macroscopic diffusion is the microscopic osmotic pressure. It arises from a lower chemical potential of the solvent on the side of a diffusing particle facing higher concentration of solutes. Molecules of the solvent rushing toward the lower chemical potential enhance the local density on the corresponding side of the particle. The resulting density gradient leads to osmotic pressure pushing the particle down the concentration gradient. This argument equally applies to a single Brownian particle for which compression and decompression density fluctuations, caused by thermal agitation, are responsible for random forces observed as irregular Brownian motion.

The notion of osmotic pressure needs clarification when applied at the molecular scale, but it provides a physically sound picture of local density augmentation as the force generation mechanism. However, electrostatics was not a part of Einstein's argument. This omission was corrected by Born in 1920.[4] He noted that dipoles changing their orientations in response to the

displacement of an ion are characterized by their own rotational relaxation times, which must cause retardation of polar response. According to fluctuation–dissipation arguments,[5] retarded response implies dissipation. This mechanism was viewed as capable of producing friction on ion's motion, which was termed the dielectric friction.[6–8]

Returning to Einstein's argument, the notion of osmotic pressure driving diffusivity and random Brownian displacements can be extended to include the interfacial polarization of a polar solvent. An asymmetric distribution of charge at the diffusing particle creates asymmetry of the electric field at different locations on the dividing surface separating the particle from the polar medium. Such unequal electric fields cause a gradient of the local chemical potential of the liquid according to the following equation[9,10] (Gaussian units):

$$\mu(E) = \mu(0) - (E^2/8\pi)(\partial\epsilon/\partial\rho)_T. \tag{1}$$

An inhomogeneous electric (Maxwell) field E compresses the liquid and alters its local dielectric constant ϵ as expressed by the isothermal density derivative $(\partial\epsilon/\partial\rho)_T$. The local chemical potential becomes spatially inhomogeneous at the particle surface, making liquid molecules rush to the region with a lower chemical potential. In electromechanics of continuous media, this physics is expressed by the Korteweg–Helmholtz force density,[9,11] which, in the absence of free charges and applied to homogeneous liquids, is given by the gradient of the chemical potential[10,12]

$$\mathbf{f}_{\mathrm{KH}} = -\rho\nabla\mu(E), \tag{2}$$

where $\mu(E)$ is from Eq. (1).

The electrostatic pull alters the local liquid density and modifies the corresponding vdW force. The electrostatic and vdW forces balance each other off (stay in peace) at mechanical equilibrium when gradients in local pressure[9,12]

$$\Delta p \simeq \Delta\left[(E^2/8\pi)\rho(\partial\epsilon/\partial\rho)_T\right] \tag{3}$$

compensate electrostatic forces from the polarized medium. The condition of mechanical equilibrium also imposes constraints on small deviations from equilibrium, leading to general statistical and dynamical relations between cross correlations of different types of forces and their self-variances, as discussed below. Understanding the statistics and dynamics of force fluctuations around equilibrium, and the role of such fluctuations in promoting diffusion, is the main focus of this Perspective.

Einstein and Born arguments concerning the physical origin of random forces acting on the diffusing particle need to be converted to closed-form relations for the translational and rotational diffusion constants. The starting point here is the Einstein equation relating the translational diffusion constant D_t to the friction coefficient ζ

$$D_t = (\beta\zeta)^{-1}, \tag{4}$$

where $\beta = (k_{\mathrm{B}}T)^{-1}$ is the inverse temperature. The rotational diffusion constant

$$D_r = (2\tau_r)^{-1} \tag{5}$$

is given[13,14] in terms of the first-rank rotational relaxation time τ_r. It is defined as the integral of the time autocorrelation function

$$C_r(t) = \langle\hat{\mathbf{u}}(t)\cdot\hat{\mathbf{u}}(0)\rangle \tag{6}$$

describing the dynamics of the unit vector $\hat{\mathbf{u}}(t)$ along the symmetry axis of a tagged particle (assuming axial symmetry for simplicity).

In contrast to the general Einstein equation that is not specific in terms of physical mechanisms of friction, the Stokes–Einstein formulation seeks the origin of translational and rotational friction in hydrodynamics. Retardation of both types of motion is viewed in terms of equations of fluid dynamics, with a common dissipation mechanism through shear viscosity η. When hydrodynamic equations are used to calculate both D_t and the rotational relaxation time τ_r for a spherical solute with the radius a, one obtains the following: $D_t = (6\pi\beta\eta a)^{-1}$ and $\tau_r = 4\pi\beta\eta a^3$. The product of D_t and τ_r depends solely on the particle size

$$D_t\tau_r = \frac{2}{3}a^2. \tag{7}$$

This is the Stokes–Einstein–Debye (SED) equation[15] and the product $D_t\tau_r$ is the SED product.

The concept of dielectric friction modifies the Stokes–Einstein paradigm. The main fundamental insight of Born's perspective is to demonstrate that hydrodynamics cannot be the sole friction mechanism for mobility in polar liquids. Dissipation of energy to rotations and translations of liquid multipoles needs to be included. Qualitative arguments incorporating polarization of the liquid–particle interface into the force balance equation clearly demonstrate that the simplistic picture of hydrodynamic friction is bound to fail for the mobility of particles carrying charges and dipoles in polar liquids. Even overall neutral colloidal particles are typically stabilized in solution by surface solvation[16] of ionic sites located close to the polar interface. In that case as well, collective fluctuations of density, dipolar orientations of polar molecules, and ions of electrolyte, mostly uncorrelated on different sides of a large colloidal particle, jointly produce random forces responsible for Brownian motion.

Analytical formulations[17] combining the Stokes–Einstein and Born friction mechanisms have been mostly based on the assumption that electrostatic and hydrodynamic forces can be viewed as statistically independent. Our discussion below shows that Born's framework substantially overestimates friction produced by a polar solvent on a small dipolar particle and on a protein molecule dissolved in water, while qualitatively correct trends are predicted for small ions. For instance, standard theories predict electrostatic friction so exceptionally high that diffusion of proteins in water is not allowed. The resolution of the paradox is found by allowing strong statistical and dynamical correlations between osmotic (vdW) and electrostatic forces acting on the diffusing particle.[18–21] The new physical reality that arises in the course of revision of basic theory assumptions also permits some simplifications and general formulas addressing the statistics of forces acting on a tagged particle. Dynamical correlations between the components forces are also very essential: they strongly reduce the relaxation time of the total force compared to relaxation of component forces.

II. DIELECTRIC FRICTION

Standard models of mobility in the Stokes–Einstein paradigm and in Born's picture both operate in terms of friction experienced by a particle drifting under an applied force. One, therefore, needs a link between thermally fluctuating forces and energy dissipation (friction). This link is provided by the fluctuation–dissipation theorem, which states that collective motions of the thermal bath coupled to a tagged particle that fluctuate the most are those that produce most friction.[22,23]

The connection between fluctuation–dissipation arguments and the friction coefficient is given by the Kirkwood equation for the translational diffusion constant D_t in terms of the fluctuating stochastic force $\mathbf{F}$ acting on the particle,[24]

$$D_t = \left[(\beta^2/3)\langle(\delta\mathbf{F})^2\rangle\tau_F\right]^{-1}. \tag{8}$$

This equation yields friction as a product of the force variance $\langle(\delta\mathbf{F})^2\rangle$, $\delta\mathbf{F} = \mathbf{F} - \langle\mathbf{F}\rangle$, and the integral relaxation time τ_F of the force–force time autocorrelation function

$$C_F(t) = \langle\delta\mathbf{F}(t)\cdot\delta\mathbf{F}(0)\rangle. \tag{9}$$

The Kirkwood equation is an approximation since the memory time should replace τ_F in the exact result.[25] Deviations from the exact formula follow from a series expansion in the square root of the ratio of the solvent and solute masses.[26] Recent molecular dynamics (MD) simulations have shown that the expansion starts with the second-order term and the first nonvanishing correction scales as the ratio of the solvent and solute masses.[27]

The total force acting on the tagged particle is a sum of the vdW and electrostatic components

$$\mathbf{F} = \mathbf{F}_{\mathrm{vdW}} + \mathbf{F}_E. \tag{10}$$

These two forces were viewed as statistically independent in the original Born formulation[4] and in many modern analytical theories of dielectric friction extending the Born model.[7,8,17,28] If vdW and electrostatic forces are statistically uncorrelated, the friction experienced by the tagged particles is additive[8,29]

$$\zeta = \zeta_{\mathrm{vdW}} + \zeta_E. \tag{11}$$

This relation breaks down dramatically for molecular solutes in water. Specific cases of spherical solutes carrying charge and dipole multipoles at the solute center are considered in sequence below to illustrate general difficulties with Born's additivity assumption leading to Eq. (11). These model cases are followed with a more general configuration of translational and rotational diffusion of an off-center ionic solute modeling diffusivity of proteins and other colloidal particles with asymmetric charge distribution. Our discussion is limited to electrostatic interactions of multipolar solutes with the polar solvent and does not include electrostatics from electrolyte ions.

A. Ion

The electrostatic force $\mathbf{F}_E = q\mathbf{E}_s$ acting from the medium on an ion carrying the charge q is the product of q and the medium electric field $\mathbf{E}_s$. The Kirkwood equation [Eq. (8)] yields the dielectric friction as a product of the electric field variance $\langle(\delta\mathbf{E}_s)^2\rangle$ and the field relaxation time τ_E,

$$\zeta_E = \frac{\beta q^2}{3}\tau_E\langle(\delta\mathbf{E}_s)^2\rangle, \tag{12}$$

where τ_E is the integral relaxation time

$$\tau_E = \int_0^\infty dt C_E(t)/C_E(0) \tag{13}$$

of the electric field time autocorrelation function

$$C_E(t) = \langle\delta\mathbf{E}_s(t)\cdot\mathbf{E}_s(0)\rangle. \tag{14}$$

The Born picture next assumes that the non-electrostatic friction is produced by non-electrostatic forces, which are statistically independent from $\mathbf{F}_E$ and can be collected into the Stokes drag. The resulting friction coefficient for translational diffusion

$$\zeta = 6\pi\eta a + \frac{\beta q^2}{3}\tau_E\langle(\delta\mathbf{E}_s)^2\rangle \tag{15}$$

applies to a liquid characterized by shear viscosity η and the ion with the radius a (stick hydrodynamic boundary conditions[2,30]). Dielectric friction carries both statistical and dynamical information in terms of the product of the force relaxation time and the force variance. It disappears if the response of molecular dipoles is very fast. A sluggish electrostatic field means more electrostatic drag imposed on an ion. As we discuss below, this result puts too much friction on a diffusing protein characterized by a slowly relaxing electric field. The assumption of components additivity in the force variance, leading to Eq. (15), needs to be revised to achieve agreement with observations.

The variance of the electrostatic field can also be connected to the field susceptibility, i.e., the ratio of the average field of the medium in response to a small probe solute dipole to the dipole magnitude.[31] This link between fluctuations and response (static limit of the fluctuation–dissipation theorem) carries the same physical meaning as the displacement variance $\langle(\delta x)^2\rangle = k_{\mathrm{B}}T/\kappa$ of a harmonic oscillator in contact with the medium at temperature T. The displacement variance is determined by the reciprocal force constant κ^{-1}, which also specifies the displacement $\Delta x = \kappa^{-1}f_{\mathrm{ext}}$ in response to a small externally applied force f_{ext}. Following the arguments advanced by Nee and Zwanzig,[17] one can define the reaction-field susceptibility[32,33] based on the field variance

$$\chi_R = \frac{\beta}{6}\langle(\delta\mathbf{E}_s)^2\rangle. \tag{16}$$

The susceptibility χ_R is accessible from solvation and spectroscopic experiments. Spectroscopy yields χ_R through the solvent-induced Stokes shift[14,34] $h\Delta\nu^{\mathrm{St}} = \Delta E^{\mathrm{St}}$ of a dipolar optical dye changing its dipole moment by Δm upon optical excitation

$$\Delta E^{\mathrm{St}} = 2\chi_R\Delta m^2. \tag{17}$$

This relation establishes direct experimental access to dielectric friction experienced by charge q,

$$\zeta_E = (\Delta E^{\mathrm{St}}/\Delta m^2)q^2\tau_E, \tag{18}$$

where τ_E can now be associated with the average relaxation time of time-resolved Stokes-shift dynamics.[14,34] The product $\tau_E \Delta E^{St}$ is given by the time integral of the unnormalized Stokes-shift time correlation function $C^{St}(t)$,

$$\tau_E \Delta E^{St} = \beta \int_0^\infty dt C^{St}(t). \tag{19}$$

The Stokes-shift correlation function describes the dynamics of the fluctuating energy gap $\Delta E(t)$ between the ground and excited states of an optical dye[35]

$$C^{St}(t) = \langle \delta\Delta E(t) \delta\Delta E(0) \rangle, \tag{20}$$

where $\delta\Delta E(t) = \Delta E(t) - \langle \Delta E \rangle$.

Equation (18) is formally exact when the linear medium response is adopted. It provides an experimental route to the electrostatic friction component. However, its usefulness for defining the mobility is limited given a strong coupling between electrostatic and non-electrostatic forces violating the assumption of their statistical independence required to arrive at Eq. (15). Nevertheless, measuring both the mobility and the Stokes-shift dynamics of a charged chromophore could be very useful in identifying key components of dielectric friction.

Solvation theories can be alternatively used to gain access to the reaction-field susceptibility through the average field $R = \langle \tilde{E}_s \rangle = 2\chi_R m$ created by the medium in response to a small dipole m placed at the solute, where $\tilde{E}_s$ refers to the solvent field projected on the direction of the solute dipole in the body frame of reference[36] (see below). The average field $\langle \tilde{E}_s \rangle$ is known as the Onsager reaction field[37] in dielectric theories.[38] The Onsager equation applies to a spherical solute with the radius a and the dipole moment m placed in the dielectric with the dielectric constant ϵ_s,

$$\chi_R^c = \frac{1}{a^3} \frac{\epsilon_s - \epsilon_\infty}{2\epsilon_s + \epsilon_\infty}, \tag{21}$$

where the superscript "c" refers to the continuum (dielectric) limit and the infinite-frequency dielectric constant ϵ_∞ accounts for the solvent electronic polarizability.

Dielectric theories[14,39] also provide the field relaxation time τ_E in Eqs. (12) and (13) in terms of the Debye relaxation time of the solvent τ_D (specified by the peak of the dielectric loss spectrum[40,41])

$$\tau_E^c = \frac{3\epsilon_\infty}{2\epsilon_s + \epsilon_\infty} \tau_D. \tag{22}$$

The combination of macroscopic hydrodynamics with macroscopic dielectric theories leads to the following equation for the translational friction coefficient within Born's framework of statistical decoupling between vdW and electrostatic fluctuating forces:

$$\zeta = 6\pi\eta a + \frac{6q^2\epsilon_\infty}{a^3} \frac{\epsilon_s - \epsilon_\infty}{(2\epsilon_s + \epsilon_\infty)^2} \tau_D. \tag{23}$$

Slightly different versions of this result were listed in classical papers by Zwanzig, Onsager and co-workers.[7,17,28]

Formulations leading to the Kirkwood equation [Eq. (8)] and dielectric solvation theories [e.g., Eq. (21)] fall under a general umbrella of the linear response approximation[17,25] (LRA) addressing the response of the medium to a weak interaction with the solute. Weakness of the solute–solvent electrostatic interaction implies little change to the medium structure induced by it. Another consequence of the LRA is the invariance of the electrostatic field variance in respect to the solute multipolar moment (charge or dipole moment).

For an ionic solute, the LRA implies independence of $\langle (\delta \mathbf{E}_s)^2 \rangle$ of the solute charge.[43] The reaction-field susceptibility χ_R in Eq. (16) must be a constant and can be calculated for a single charge state of the ion. This turns out to be mostly correct when the ionic charge of a Lennard-Jones (LJ) solute in SPC/E water is varied in the range $-3 \le (q/e) \le 3$ in MD simulations[42] [Fig. 1(a)]. The agreement is nearly perfect for anions, but an increase in χ_R above the LRA prediction is seen for cations. This is related to restructuring of the hydration shell around a cation pulling water's oxygens closer to the solute and forcing the corresponding O–H bonds to reorient into the bulk. The ability of the dielectric theories [Eq. (21)] to estimate χ_R is strongly affected by the definition of the ionic radius a. When the microscopic solute–solvent density profile is incorporated in a microscopic solvation theory, the agreement with MD is very good in the range of charges where LRA still holds[33] [dashed line in Fig. 1(a)].

The field relaxation time τ_E is also supposed to be independent of the ionic charge in the LRA framework. τ_E from MD simulations mostly follows the prediction of dielectric theories [Eq. (22)] for spherical ions, as indicated by filled circles and the dashed line in Fig. 1(b). Both τ_E and the relaxation time of the total force τ_F are nearly independent of the ionic charge, as anticipated by the LRA. This outcome is drastically distinct from a strong retardation of rotational and field dynamics with increasing magnitude of the solute dipole discussed below. The relaxation time τ_F is the

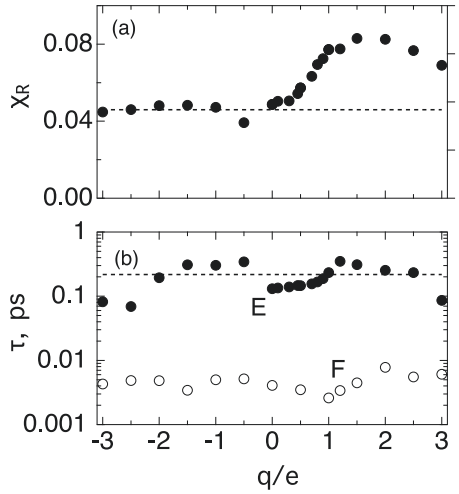

FIG. 1. (a) The reaction-field susceptibility χ_R [Eq. (16)] from MD simulations[42] of Lennard-Jones ions in SPC/E water vs the ionic charge q. The horizontal dashed line marks the microscopic calculation from Ref. 33. (b) Relaxation times of the electric field τ_E [Eq. (13), filled circles, E] and the total force τ_F [Eq. (9), open circles, F]. The dashed line indicates the dielectric relaxation time τ_E^c from Eq. (22). Reprinted with permission from J. Chem. Phys. **156**, 204501 (2022). Copyright 2022 AIP Publishing LLC.[42]

integral relaxation time for the force correlation function $C_F(t)$ in Eq. (9). Importantly, τ_F is significantly lower than τ_E. This outcome implies strong dynamic correlations between vdW and electrostatic forces making the overall force much faster than the component forces. This result becomes particularly prominent for translational mobility of proteins discussed below.

A weak dependence of τ_F on q [Fig. 1(b)] implies that the dependence of translational diffusion on the ionic charge must arise from the force variance. The Born picture suggests that a linear dependence of $D_t^{-1}(q)$ on q^2 comes from the electrostatic force variance [Eq. (15)]. A more general view in terms of the Kirkwood equation includes all three terms entering the force variance through Eqs. (8) and (10),

$$\langle(\delta\mathbf{F})^2\rangle = \langle(\delta\mathbf{F}_E)^2\rangle + \langle(\delta\mathbf{F}_{\rm vdW})^2\rangle + 2\langle\delta\mathbf{F}_E\cdot\delta\mathbf{F}_{\rm vdW}\rangle. \quad (24)$$

In contrast to the Born assumption, assigning the term $\propto q^2$ in Eq. (23) to the electrostatic force, MD simulations show that all terms in Eq. (24) scale linearly with q^2 for simple LJ ions in SPC/E water (Fig. 2). A surprisingly simple result was found to hold for the vdW-E cross-correlation term for small dipolar solutes,[44] proteins,[45,46] and colloidal nanoparticles.[47] The cross-correlation is negative and nearly coincides in magnitude with the electrostatic force variance

$$\langle\delta\mathbf{F}_E\cdot\delta\mathbf{F}_{\rm vdW}\rangle \simeq -\langle(\delta\mathbf{F}_E)^2\rangle. \quad (25)$$

From this formula, the variance of the total force acting on a tagged particle comes as the result of subtraction of the vdW and electrostatic self-components

$$\langle(\delta\mathbf{F})^2\rangle \simeq \langle(\delta\mathbf{F}_{\rm vdW})^2\rangle - \langle(\delta\mathbf{F}_E)^2\rangle. \quad (26)$$

This equation replaces the additivity of self-variances in the Born picture leading to Eqs. (11) and (15).

The empirical result of Eq. (25) holds well for LJ cations as shown in Fig. 2. On the other hand, the asymmetry between anionic and cationic solvation[48–50] leads to a somewhat different result for LJ anions[46]

$$\langle(\delta\mathbf{F})^2\rangle \simeq \langle(\delta\mathbf{F}_{\rm vdW})^2\rangle. \quad (27)$$

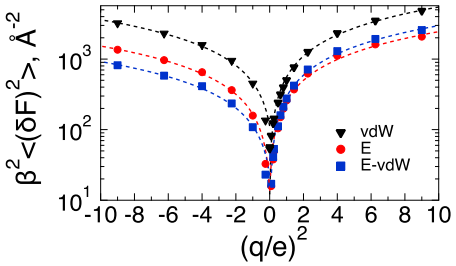

FIG. 2. Components of the force variance $\beta^2\langle(\delta\mathbf{F}_a)^2\rangle$, a = E, vdW vs q^2: vdW (black triangles), electrostatic (red circles), and the negative of cross vdW-electrostatic (blue squares).[42] The results for anions are plotted vs $-q^2$. The dashed lines are linear fits through the points (note the logarithmic scale). Adapted with permission from J. Chem. Phys. **156**, 204501 (2022). Copyright 2022 AIP Publishing LLC.[42]

Nevertheless, both anions and cations maintain a linear scaling of $D(q)^{-1}$ with q^2: diffusion becomes slower for charged ions because of a rising variance of the total force acting on the solute.

An increase in the vdW variance with the ionic charge is a consequence of compression of the hydration shell induced by the ion. Anions are more efficient in compressing water since closer packing and higher density are achieved in this case by releasing dangling O–H bonds[51] pointing toward the negative charge of the ion. Distinct shell compression between cations and anions leads to solvation asymmetry[48–50] and extends to asymmetry of linear transport coefficients: according to the Kirkwood equation, cations should diffuse faster than anions of the same size and charge magnitude.

B. Dipole

Solutes with asymmetric distribution of molecular charge might carry multipolar moments, most importantly the dipole moment. Dielectric friction affects both translational and rotational[17,52,53] diffusion for these charge configurations. We start with simple arguments explaining why electrostatic effects can discriminate between translational and rotational dynamics. This distinction leads to a substantial violation of the SED equation [Eq. (7)] in high-temperature polar solvents.

Random torques is the source of rotational diffusion and friction imposed by the medium on a tagged dipole **m**. Following the fluctuation–dissipation arguments discussed above, stronger torque fluctuations mean higher rotational friction. The electric component of the torque is caused by the electric field $\mathbf{E}_\perp$ perpendicular to the dipole (Fig. 3)

$$\mathbf{T}_E = \mathbf{m}\times\mathbf{E}_s. \quad (28)$$

Thermal fluctuations of $\mathbf{E}_\perp$ cause random rotations, and the time scale of field relaxation sets up the dissipation mechanism. This phenomenology is fully analogous to Born's model for ionic translations. The rotational relaxation time of a dipole τ_r retraces[17] Eq. (15) for translational diffusion of an ion once the assumption of statistical independence between vdW and electrostatic forces is adopted,

$$\tau_r = \tau_r^0 + \frac{(\beta m)^2}{6}\tau_E\langle(\delta\mathbf{E}_s)^2\rangle. \quad (29)$$

Here, τ_r^0 is the relaxation time related to random torques of non-electrostatic origin. The coefficient of rotational diffusion D_r of a molecule with axial symmetry[13] follows from τ_r according to Eq. (5).

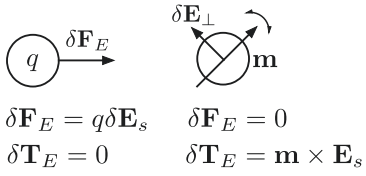

FIG. 3. Effect of electrostatic solute–solvent interactions on a spherical ion (charge q) and a spherical dipole (dipole moment **m**). There is a fluctuating electrostatic force $\delta\mathbf{F}_E$ acting on the ion, but there is no electrostatic torque. In contrast, the force acting on the dipole is zero, but there is a nonzero electrostatic torque inducing rotations if the solvent field has a projection $\delta\mathbf{E}_\perp$ perpendicular to the dipole **m**.

When dielectric theories are used for the reaction-field susceptibility [Eq. (21)] and the field relaxation time [Eq. (22)], the rotational time becomes

$$\tau_r^c = \tau_r^0 + \tau_D \frac{3\beta m^2 \epsilon_\infty}{a^3} \frac{\epsilon_s - \epsilon_\infty}{(2\epsilon_s + \epsilon_\infty)^2}. \tag{30}$$

In addition, the link between the reaction-field susceptibility χ_R and the Stokes-shift dynamics[14,34] [Eqs. (17) and (19)] relates the increment in the rotational time $\Delta\tau_r = \tau_r - \tau_r^0$ caused by electrostatics to the Stokes shift dynamics[31]

$$\Delta\tau_r = \frac{m^2}{2\Delta m^2} \beta \Delta E^{\mathrm{St}} \tau_E, \tag{31}$$

where $\Delta E^{\mathrm{St}}\tau_E$ is given by Eq. (19).[53,54]

Equation (31) offers two significant advantages over Eq. (30). First, no specific solvation model is required. Second, corrections of the dipole moment due to chromophore's polarizability[53,55] cancel out in the ratio $m^2/\Delta m^2$. A linear relation $\Delta\tau_r \propto \Delta E^{\mathrm{St}}\tau_E$ was indeed observed experimentally.[53,55,56] However, the linear slope was found to be grossly inconsistent with expectations based on the known dipole moments. This dramatic failure was related to the breakdown of the assumption of friction additivity inherent to the Born picture [Eqs. (11) and (15)] and to its extension[17] in terms of Eq. (30). Strong cross correlations between vdW and electrostatic torques have also been detected by MD simulations.[44,57]

The vdW-electrostatic cross correlations are significant for the torque variance

$$\langle(\delta\mathbf{T})^2\rangle = \langle(\delta\mathbf{T}_E)^2\rangle + \langle(\delta\mathbf{T}_{\mathrm{vdW}})^2\rangle + 2\langle\delta\mathbf{T}_E \cdot \delta\mathbf{T}_{\mathrm{vdW}}\rangle. \tag{32}$$

Simulations of diatomic solutes composed of two fused LJ spheres with charges $\pm q$ placed at their corresponding geometric centers[44] (Fig. 4) have shown that the remarkable relation connecting cross correlation of force components to the electrostatic self-variance [Eq. (25)] extends to torques (Fig. 5)

$$-\langle\delta\mathbf{T}_E \cdot \delta\mathbf{T}_{\mathrm{vdW}}\rangle \simeq \langle(\delta\mathbf{T}_E)^2\rangle. \tag{33}$$

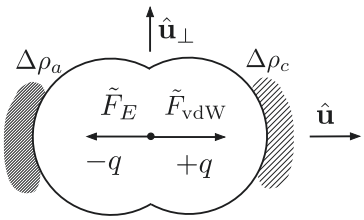

FIG. 4. Schematic drawing of the fused dumbbell diatomic with charges $\pm q$ placed at the geometric centers of two Lennard-Jones spheres. The shaded areas are parts of the water shell structurally arrested by electrostatic pull from the charge sites. The anionic end of the solute produces a denser hydration shell $\Delta\rho_a$ compared to the cation with $\Delta\rho_c$. The average vdW and electrostatic forces in the body frame are along the symmetry axis indicated with the unit vector $\hat{\mathbf{u}}$. The orthogonal direction is indicated with the unit vector $\hat{\mathbf{u}}_\perp$.

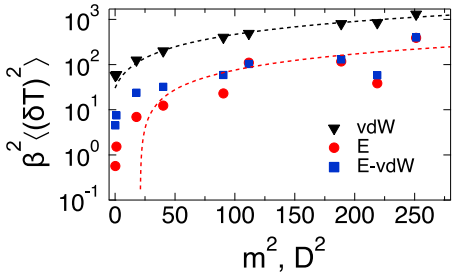

FIG. 5. Variances of torques acting from water on fused dumbbell solutes with varying charge $\pm q$ placed at two LJ centers (Fig. 4). MD results[44] show the vdW (black triangles) and electrostatic (red circles) self-variances and the negative of the vdW-electrostatic cross correlations (blue squares) vs the solute dipole moment squared. The dashed lines are linear fits through the points (note the logarithmic scale).

The variance of the torque acting on the dipole comes as subtraction of the vdW and electrostatic self-components in close analogy to Eq. (26),

$$\langle(\delta\mathbf{T})^2\rangle \simeq \langle(\delta\mathbf{T}_{\mathrm{vdW}})^2\rangle - \langle(\delta\mathbf{T}_E)^2\rangle. \tag{34}$$

One can observe from Fig. 5 that Eqs. (33) and (34) are satisfied only for sufficiently high solute dipole moments. Therefore, compensation relations for forces and torques apply only when the hydration shell of an ion or a dipole is sufficiently altered by the electrostatic pull of the solute. The result of this modification is the formation of a thin, structurally arrested layer of the solvent at the solute surface. This layer is distinct from Frank–Evans iceberg model[58] introduced to account for the loss of entropy in hydrophobic solvation. In this view, water molecules around a hydrophobic solute are translationally constrained by a strong interfacial network of hydrogen bonds producing a cage. In contrast, the arrested structure invoked here applies only to the orientational manifold: the water molecules nearly freely exchange with the bulk but arrive to the arrested layer with the distribution of orientations dictated by the local electrostatic fields. A similar picture has emerged in the problem of the loss of dielectric strength by interfacial water (see below): the surface layer displaying lower dielectric susceptibility is arrested only in terms of orientations of water molecules. Their translational mobility is nearly unaffected and they keep exchanging with the bulk.[59] To sum up, only orientations of the solvent molecules are affected in the thin surface layer rotating together with the solute. This physical picture provides a qualitative explanation for the compensation relations. It can be converted to mathematical arguments that provide a plausible explanation of the simulation results and can potentially lead to the development of a rigorous theory.

To understand the origin of compensation relations, one has to distinguish the component forces in the frame of the solute (body frame, marked with tildes) and in the laboratory frame (without tildes). If one assigns the unit vector $\hat{\mathbf{u}}$ along the symmetry axis of the solute (assuming axial symmetry for simplicity), the force components $\tilde{F}_a$ (a = vdW, E) projected on $\hat{\mathbf{u}}$ in the body frame will rotate with the solute in the laboratory frame. Fluctuations of the force in the laboratory frame become a sum of rotations of the average force and fluctuations of the body-frame force

$$\delta\mathbf{F}_a = \langle\tilde{F}_a\rangle\hat{\mathbf{u}} + \delta\tilde{\mathbf{F}}_a. \tag{35}$$

The fluctuations occur around the total average force applied from the solvation layer to the solute and directed along the solute symmetry axis in the body frame

$$\langle\tilde{F}\rangle = \langle\tilde{F}_E\rangle + \langle\tilde{F}_{\rm vdW}\rangle. \tag{36}$$

This situation is illustrated in Fig. 4 for a diatomic dumbbell made of two fused LJ spheres with opposite charges $\pm q$ placed at their geometrical centers.[44] Even though the radii of two spheres are equal, the asymmetry in the compression of the water shell next to the positive and negative ends of the solute (shown with the shaded areas) creates nonzero vdW and electrostatic forces in the body frame.

Assume next that the total force in the body frame $\langle\tilde{F}\rangle$ is zero (we show below that this is not always the case) and that the arrested molecular orientations in the solvation shell do not allow fluctuations of the electrostatic force in the body frame ($\delta\tilde{\mathbf{F}}_E = 0$). The electrostatic fluctuations observed in the laboratory frame (without tildes) are only allowed through random rotations of the unit vector $\hat{\mathbf{u}}$ specifying the solute orientation and one can write

$$\delta\mathbf{F}_E = \langle\tilde{F}_E\rangle\hat{\mathbf{u}}. \tag{37}$$

At $\langle\tilde{F}\rangle = 0$, the average projection of the vdW force along $\hat{\mathbf{u}}$ balances $\langle\tilde{F}_E\rangle$. Since fluctuations of density are allowed in the solvation shell, they will produce fluctuations of the vdW force both along $\hat{\mathbf{u}}$ and in the direction $\hat{\mathbf{u}}_\perp$ orthogonal to $\hat{\mathbf{u}}$ (see Fig. 4),

$$\delta\mathbf{F}_{\rm vdW} = -\langle\tilde{F}_E\rangle\hat{\mathbf{u}} + \delta F_{\rm vdW}\hat{\mathbf{u}} + \delta F^{\perp}_{\rm vdW}\hat{\mathbf{u}}_\perp. \tag{38}$$

The compensation relation [Eq. (25)] immediately follows when this condition is satisfied. This formula also ensures $\langle(\delta\mathbf{F}_{\rm vdW})^2\rangle > \langle(\delta\mathbf{F}_E)^2\rangle$ required for the overall force variance to be positive in Eq. (26). The assumption that electrostatic forces from the arrested layer show no fluctuations in the body frame is therefore sufficient to explain the compensation result. While these mathematical arguments are consistent with statistical averages produced by MD simulations, a fully quantitative theory of the compensation phenomenon is still missing.

The formation of a tightly bound interfacial layer is also reflected in changes of the electric-field relaxation time τ_E with the solute dipole m. The relaxation time τ_E shows very little change with the ionic charge q [Fig. 1(b)] since the rotations are irrelevant for a spherically symmetric ion. A very different result is found for the dipole in SPC/E water:[44] τ_E increases linearly with m^2 and reaches the retardation factor of ~800 in the range of dipole moments shown in Fig. 6. A structurally arrested water layer slows down both the rotational and field dynamics. This is, in fact, expected since Eq. (37) also stipulates the following relation between the electric field [Eq. (6)] and rotational [Eq. (14)] time correlation functions:

$$C_E(t) = \langle\tilde{F}_E\rangle^2 C_r(t). \tag{39}$$

A good match between τ_E and τ_r required by this formula was indeed found in MD simulations of solutes carrying large dipole moments[44] and off-center charges.[46]

Adding dipolar solutes to a polar liquid also strongly affects the solution viscosity.[60,61] Even though viscosity can be a nonlinear function of the solute concentration, the rotational relaxation time of the solute is often found to follow the standard hydrodynamic predictions.[60] These observations are challenging to both the traditional theories of dielectric friction and to the more recent simulation results discussed here. There is still room for an extension of theories of rotational diffusion to connect to experimental measurements of solution viscosity.

From the experimental standpoint, the retardation effect of the solute dipole on the electric field dynamics translates to slower Stokes-shift dynamics for excited-state chromophores[35,62] usually carrying higher molecular dipoles. This observation also suggests slower field and rotational dynamics in highly polar liquids and slower field dynamics inside solutes carrying large dipole moments, such as solvated proteins discussed below.

Bulk water is a good example of this general phenomenology. Simulations[44] of $\tau_E(T)$ of SPC/E water at different temperatures are compared in Fig. 7 to the continuum result from Eq. (22) and to the Debye relaxation time $\tau_D(T)$ from simulations[63] and experiment.[64] The Nee–Zwanzig equation for rotational dielectric friction [Eq. (29)] strongly overestimates the rotational time for water molecules confirming again that the neglect of vdW-electrostatic correlations is not justified for rotational dynamics in bulk polar liquids. At the same time, the continuum estimate $\tau_E = \tau_E^c$ [Eq. (22)]

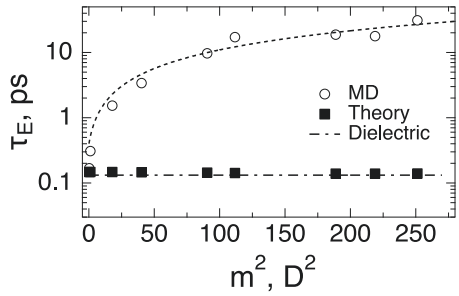

FIG. 6. Relaxation time τ_E calculated from MD simulations[44] (open points) and from the microscopic solvation theory[33] (filled points). The dashed-dotted line refers to the dielectric formula in Eq. (22). The dashed line is a linear fit through the MD points (note the logarithmic scale): $\tau_E = 0.230 + 0.106 \times m^2$ ps, and m is in D.

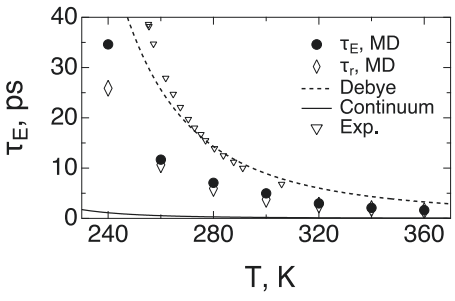

FIG. 7. τ_E from MD simulations[44] at different temperatures (filled circles) compared to the Debye relaxation time τ_D of SPC/E water[63] (dashed line, Debye) and to the continuum estimate of the relaxation time τ_E^c from Eq. (22) (solid line, Continuum). Also shown are single-molecule rotational relaxation times τ_r [Eq. (6)] (open diamonds)[65] and experimental Debye relaxation times[64] $\tau_D(T)$ (open triangles).

falls much below τ_E from MD simulations. This outcome comes in stark contrast to a reasonable performance of dielectric theories in estimating τ_E for spherical LJ ions [Fig. 1(b)].

The phenomenology of a dipole rotating together with its arrested solvation layer is responsible for the failure of dielectric theories when applied to the electric field dynamics. The relaxation time deviates significantly upward from $\tau_E^c(T)$ approaching $\tau_D(T)$.[63,64] It is important to note that single-particle rotational dynamics of water are non-diffusional, involving a sequence of jumps activated by rearrangement of hydrogen bonds to the nearest neighbors.[66] Nevertheless, relaxation of electric field is a collective process, similarly to the Debye dielectric relaxation,[67] and should average out individual molecular jumps through participation of many water molecules. Simulations still find a good match between the rotational,[65] τ_r, and field, τ_E,[44] relaxation times (compare filled circles to open diamonds in Fig. 7) in support of Eq. (39). An equally good match was found in MD simulations of glycerol[68] [Fig. 8; the solid line indicates dielectric $\tau_D(T)$ data[69]]. This match extends through the dynamical crossover signaled by a change in the Arrhenius slope of the relaxation time also observed in recent scattering experiments for glycerol,[70] although at longer times. One anticipates that the Debye picture of rotational diffusion[71] made of small rotational jumps applies better to glycerol than to water, but the phenomenology $\tau_r \simeq \tau_E$ [Eq. (39)] seems to hold for both hydrogen-bonding liquids.

The single-particle rotational relaxation time τ_r can also be linked to the collective Debye relaxation time τ_D. The connection in terms of the static Kirkwood correlation factor[38] $g_K(T)$ was introduced long ago by Keyes and Kivelson[72] and Kivelson and Madden,[73]

$$\tau_D(T) = g_K(T)\tau_r(T). \tag{40}$$

The derivation of this equation involves some approximation and it has long remained a conjecture. However, recent experiments[74,75] and MD simulations[76,77] have produced evidence in support of its accuracy. Also MD simulations of relaxation times and Kirkwood factors of SPC/E and TIP3P water models at different temperatures have attested to its high accuracy.[65]

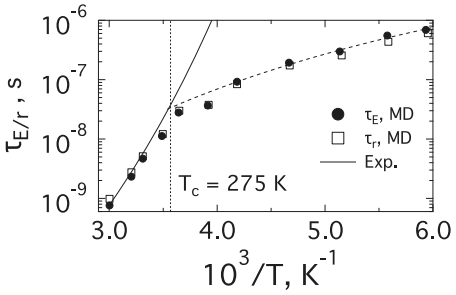

FIG. 8. Relaxation times τ_r and τ_E from MD simulations of glycerol. The solid line refers to the dielectric relaxation time[69] $\tau_D(T)$ obtained by fitting dielectric loss spectra at different temperatures to the Cole–Davidson function. The dashed line is a regression drawn through τ_E points. T_c (dotted vertical line) indicates the crossover temperature at which the Arrhenius slope changes. Adapted with permission from S. Seyedi, D. R. Martin, and D. V. Matyushov, Phys. Rev. E **94**, 012616 (2016). Copyright 2016 American Physical Society.[68]

C. SED violation

Retardation of translational and rotational dynamics by dielectric friction affects yet another iconic result of single-particle dynamics in liquids, the SED equation[15,78–82] [Eq. (7)]. The effect of electrostatics on translational and rotational diffusion must be entirely different for a spherical ion and a spherical dipole. Figure 3 illustrates the distinction for two spherical solutes: (i) an ion with charge q at its center and (ii) a point dipole **m** at the solute center. Fluctuations of the electrostatic force applied to an ion contribute a term $\propto q^2$ to translational friction [Eq. (15)], but there is no electrostatic torque. Electrostatics, thus, affects D_t of an ion but does not affect τ_r and one anticipates violation of the SED relation. Just an opposite situation applies to a point dipole. If the electric field is uniform within the solute, there is no electrostatic force, but there is an electrostatic torque responsible for retardation of rotations. One anticipates deviations from hydrodynamics for τ_r while maintaining D_t consistent with hydrodynamics.

SED violation was indeed found in MD simulations of dipolar solutes in SPC/E water.[44] Instead of being a constant, as predicted by Eq. (7), the SED product becomes a linear function of m^2, where m is the solute dipole moment. The dependence of the SED product on temperature is even more instructive.

The strength of the dipole–water electrostatic interactions enters the system partition function through the dimensionless parameter $(m^*)^2 = \beta m^2/\sigma_{0s}^3$, where σ_{0s} is the solute–solvent interaction distance, which is typically slightly below the position of the first peak of the solute–solvent pair distribution function. The dimensionless interaction parameter m^* can be increased by either increasing the solute dipole, as is done in simulations and in optical excitation experiments, or by lowering temperature. For a dipolar solute, simulations indicate a sharp rise of the SED product with lowering temperature following a plateau region at higher temperatures (Fig. 9). Such a kink in the temperature dependence of the SED product is often reported for single-particle dynamics of supercooled molecular glass-formers.[79,82,83]

SED violation is often attributed to heterogeneous dynamics,[79,81,84,85] i.e., temporal coexistence of domains with fast and slow dynamics in a homogeneous medium. Dynamic heterogeneity becomes a signature of nonergodicity in respect to measurements of structural α-relaxation. Distributed α-relaxation times, leading to dispersed dynamics,[81,83,84] are a consequence of

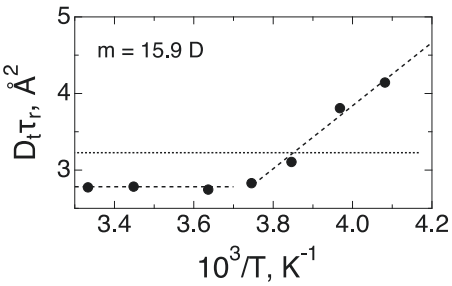

FIG. 9. SED product [Eq. (7)] vs inverse temperature for a fused dumbbell solute (Fig. 4) with the dipole moment listed in the plot.[44] The points denote MD simulation results, and the dashed lines are linear fits through the corresponding portions of data. The dotted line refers to the hydrodynamic SED product in Eq. (7).

a slower dynamical process relaxing heterogeneous domains and restoring ergodicity on a time scale much longer than the time of α-relaxation. SED violation is then explained by the observation that translational diffusion is dominated by fast states, while slow states mostly contribute to rotational diffusion[84] (this view was disproved in simulations of SPC/E water[82]). There are obviously no such distributed states in simulations of a single solute, but SED product still increases either with increasing the solute dipole moment or with lowering temperature (Fig. 9). Electrostatic interactions, which increase in importance with lowering temperature, might offer an alternative explanation for SED violation.

III. COMPLEX MOLECULAR/COLLOIDAL SOLUTES

The configuration of a spherical ion considered in the original work of Born and carried over to many subsequent studies is highly unrealistic when applied to large molecular solutes. For a charged solute, such as a solvated protein, atomic charges are distributed inside the molecule and over its surface. The center of charge often does not coincide with the molecular center of mass. The solute electric field is anisotropic and the interfacial polarization produces both the electrostatic force affecting center-of-mass translations and torques inducing rotations. Translations and rotations become highly coupled, through the electrostatic solute–solvent interactions, with the observable consequences discussed here.

When the center of molecular charge is shifted relative to the center of mass, as is illustrated in Fig. 10, the imbalance of the chemical potential on different sides of the particle is caused by asymmetry of the electric field [Eq. (1)]. The gradient of the chemical potential is compensated by density augmentation leading to the vdW force directed oppositely to the electrostatic force (compare to Fig. 4). If one now assigns the unit vector $\hat{\mathbf{u}}$ to the z-axis in the body frame connecting the center of mass to the center of charge, one can write the force components $\tilde{F}_a$ ($a = \mathrm{vdW}, \mathrm{E}$) measured in the body frame

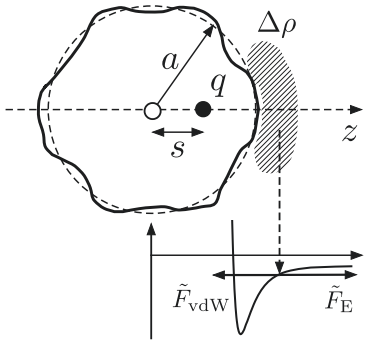

FIG. 10. Schematic drawing of a colloidal particle with the center of mass marked with an open dot and the center of charge q with the filled dot; s is their separation. An asymmetric electrostatic field induces the electrostatic force $\tilde{F}_E$ and a density augmentation $\Delta\rho$ responsible for the van der Waals (vdW) force $\tilde{F}_{\mathrm{vdW}}$ in the body reference frame with the z-axis along the line connecting centers of mass and charge. The lower portion schematically shows the solute–solvent vdW interaction potential. The vdW and electrostatic forces are balanced off for the solvent molecules in the interface; a is the radius of the sphere representing the solute (dashed line).

rotating with the solute according to Eq. (35). Fluctuations of forces in the laboratory frame become sums of rotations of the average force and fluctuations of the body-frame forces.

The average electrostatic force along the z-axis in the body frame can be calculated by surface integration of the Maxwell stress tensor $T_{z\beta}$, contracted with the Cartesian components $\hat{n}_\beta$ of the outward unit vector normal to the surface[9,10,86]

$$\langle \tilde{F}_E \rangle = \oint T_{z\beta}\hat{n}_\beta dS, \tag{41}$$

where dS is the surface area differential and summation runs over the common Cartesian indices. Dielectric theories used to estimate the integral in Eq. (41) yield[9,46] the body-frame electrostatic force in the form

$$\langle \tilde{F}_E \rangle \propto \frac{sq^2}{\epsilon^2 a^3}\left[\epsilon + \rho\left(\frac{\partial\epsilon}{\partial\rho}\right)_T\right], \tag{42}$$

where s is the distance between the centers of mass and charge (Fig. 10). The physical reason for this result is that liquid dipoles are drawn to the region with a higher electric field as long as liquid's compressibility permits a density contraction. The force is caused by changes of the dielectric constant by interfacial density contraction. The derivative $\rho(\partial\epsilon/\partial\rho)_T$ is close in magnitude to ϵ for many polar liquids,[12] and the force in Eq. (42) scales as $\propto \epsilon^{-1}$ with the dielectric constant when $\epsilon \gg 1$. Equation (42) is derived assuming that no tangential electrostatic stress is allowed at the particle surface. If both the tangential and normal stresses are allowed, the term in the brackets in Eq. (42) is replaced by $\rho(\partial\epsilon/\partial\rho)_T$.

The question of what is the dielectric constant to be used in Eq. (42) is far from trivial. A number of recent computer simulations[59,87,88] and experiments[89,90] have shown that an effective dielectric constant, significantly reduced compared to the bulk, is required to characterize interfacial polarization of water and other liquids.[91] The exact reduction from the bulk value of $\epsilon \simeq 78$ for water at standard conditions has not been established, but values in the range $\simeq$ 2–10 have been reported. Comparing the electrostatic force from MD simulations of a solute with the off-center charge (Fig. 10) to Eq. (42) requires[46] $\epsilon \simeq 5$, which is consistent with the anticipated reduction of the interfacial dielectric response.[92]

If the hydration shell is in mechanical equilibrium, vdW and electrostatic forces in the laboratory frame average out to zero such that $\langle \tilde{F}_E \rangle = -\langle \tilde{F}_{\mathrm{vdw}} \rangle$. When applied to Eq. (35), this assumption leads to Eq. (38) and the compensatory relation between cross and self-variances [Eq. (25)]. This is indeed found in simulations of charge mutants of proteins for which the compensation relation [Eq. (25)] is satisfied with great accuracy.[45] The distributions of the body-frame force components shown in Fig. 11(a) for the $q = -2$ mutant of azurin are shifted symmetrically around zero overall force but show different widths required to reach an overall nonzero variance in Eq. (26). Such an exact compensation does not, however, occur for a spherical LJ solute with an off-center charge dissolved in SPC/E water.[46] The vdW force in this case is both greater on average and produces a greater force variance. The average force along the symmetry axis of the solute is nonzero in the body frame, but it averages out to zero by solute rotations in the laboratory frame. The total solute–solvent force is zero in the laboratory frame at sufficiently long observation times as required for mechanical equilibrium.

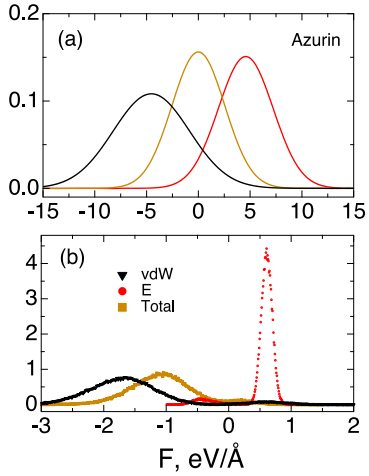

FIG. 11. Normalized distributions of vdW (black), electrostatic (red), and total (mustard) force projected on the symmetry axis of azurin protein carrying the charge $q = -2e$ [oxidized state (a)] and of a spherical LJ solute with the off-center charge $q = 1.5e$ (b). Adapted with permission from T. Samanta, S. M. Sarhangi, and D. V. Matyushov, J. Phys. Chem. Lett. **12**, 6648 (2021). Copyright 2021 American Chemical Society.[46]

The existence of a nonzero average force in the solute body frame leads to non-Gaussian force statistics in the laboratory frame because the average force component $\langle \tilde{F}_a \rangle$ (a = vdW, E) rotates with the solute. This is illustrated in Fig. 12 for the distribution of the electric field from SPC/E water at the center of a dumbbell solute shown in Fig. 4.[44] The Gaussian distribution in the body frame is transformed, by rotations of the solute, to a step-wise distribution in the laboratory frame. It arises from all possible orientations of the Onsager reaction field $R = \langle \tilde{E}_s \rangle$ indicated by the position of the distribution peak in the body frame (Fig. 12). Any observable property sensitive to the electric field in the laboratory frame should be affected by this non-Gaussian statistics.

An illuminating application of this general result is a long-known observation that an ensemble of independently rotating dipoles yields a non-zero nonlinear dielectric response experimentally observed through the dependence of the dielectric constant on the applied electric field.[38] This effect, which requires non-Gaussian statistics of the macroscopic dipole moment of the sample,[41] is allowed by non-Gaussian statistics of individually rotating dipoles.

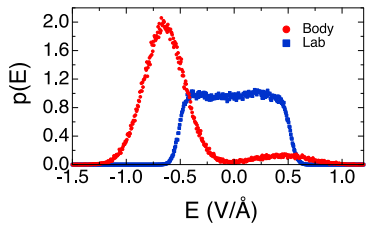

FIG. 12. Distributions of the electric field created by SPC/E water (T = 300 K) at the geometrical center of a fused dumbbell solute (Fig. 4) in the laboratory (blue squares) and body (red circles) frames of reference. The MD results refer to charges $q = \pm 1.5e$ placed at two geometric centers of a fused LJ diatomic.[44]

The remarkable accuracy of the compensation relation [Eq. (25)] found for proteins[45] suggests a strong correlation between vdW and electrostatic forces driving translational and rotational diffusion. We have already noted the failure of dielectric friction theories in describing rotations of molecular dipoles in bulk water (Fig. 6). For proteins, the failure of traditional theories is particularly dramatic.

Dielectric friction is estimated in standard theories in terms of the product of the electric field variance and the field relaxation time [Eqs. (15) and (29)]. For proteins, the field relaxation time turns out to be substantially longer than the dielectric time $\tau_E^c \simeq 0.3$ ps in Eq. (22). This can be anticipated already from the results for a model dipolar solute shown in Fig. 6, where the retardation factor of ~180 was reached for the largest dipole moment ≃ 15 D. Dielectric experiments have shown that proteins carry large dipole moments of the order of several hundreds of Debye units as defined relative to the center of mass for proteins possessing net charge.[95–97] Such large dipoles cause nonlinear retardation of the electric field dynamics from the subpicosecond domain predicted by dielectric theories [Eq. (22)] and confirmed for simple ions [Fig. 1(a)] to the nanosecond time domain shown for three globular proteins[93,94] in Fig. 13. The retardation factor of the electric field dynamics reaches an astonishing value of four orders of magnitude for proteins.

The correlation functions $C_E(t)$ [Eq. (14)] in Fig. 13 were determined in the frame of the simulation box (laboratory frame). Consistent with Eq. (39), the long-time decay of $C_E(t)$ parallels the rotational correlation function $C_r(t)$ (black triangles in Fig. 14). The decay of the correlation function is somewhat faster, and the relaxation time is somewhat lower in the body frame (Fig. 14), but still significantly exceeds τ_E^c and the results for simple ions. Spectroscopic, optical or vibrational,[98] probes sensitive to the solvent-induced electric field (solvatochromism) rotate together with the protein and thus report on the field dynamics and statistics in the body frame. In contrast, rotational and translational diffusion are affected by the dynamics and statistics of the solvent electric field in the laboratory frame of reference.

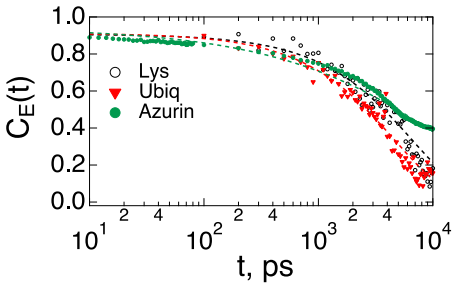

FIG. 13. Normalized time correlation functions $C_E(t)/C_E(0)$ [Eq. (14)] of the electric field from water at the center of mass of the protein calculated from 1 μs MD trajectories of lysozyme (Lys, black circles) and ubiquitin (Ubiq, red triangles).[93] The dashed lines are fits to weighted sums of exponential and stretched exponential decay functions. Also shown is the time correlation function of the electric field at the active site of the oxidized form of azurin (green circles, Azurin).[94] The average relaxation times are 6.3 ns (Lys), 4.4 ns (Ubiq), and 8.5 ns (Azurin). Adapted with permission from M. Heyden and D. V. Matyushov, J. Phys. Chem. B **124**, 11634 (2020). Copyright 2020 American Chemical Society.[93]

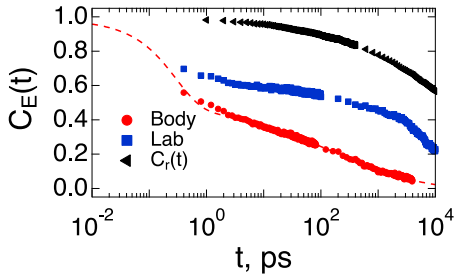

FIG. 14. Normalized time correlation functions $C_E(t)/C_E(0)$ [Eq. (14)] of the electrostatic force acting from water on azurin in the reduced state[45] in the laboratory (blue squares) and body (red circles) frames. The integral relaxation times are τ_E = 6.7 ns (lab) and τ_E = 1.1 ns (body). The dashed line is a fit to a weighted sum of single exponential and stretched exponential relaxation functions. Also shown is the normalized rotational time correlation function[45] [black triangles, Eq. (6)].

A dramatic signature of slow electric field dynamics in proteins is seen in a sharp decrease of the bandwidth of vibrational lines of spectroscopic probes placed inside proteins compared to the same probes dissolved in water.[98,99] The overall broadening, due to electric field fluctuations, is similar in water and in protein. However, much slower dynamics of the electric field inside the protein do not allow reaching full equilibrium line broadening on the lifetime of the vibrational probe.[94]

When relaxation the time τ_E and the field variance $\langle(\delta \mathbf{E}_s)^2\rangle$ specific for proteins are used in Eq. (15), one finds that electrostatic friction exceeds the hydrodynamic friction by a factor of $\simeq 10^6$. The standard theories of dielectric friction, thus, prohibit protein diffusion in water. Direct simulations of protein mutants show essentially no dependence of translational diffusivity on the net protein charge,[45] in agreement with experimental evidence.[100–103]

The failure of standard recipes comes from the neglect of vdW-electrostatic correlations, which impact both the force statistics and dynamics. First, instead of additivity of the component variances, one obtains their subtraction in the total force variance [Eq. (26)]. Second, and more important, relaxation of the total force [Eq. (10)] is much faster than relaxation of the component forces (Fig. 15). The total force decays, through oscillations, on the time scale of $\simeq$ 0.01 ps, while relaxation of the vdW and electrostatic forces occurs on the time scale of 5–6 ns (note the logarithmic scale in Fig. 15). The component forces are retarded compared to the total force by nearly six orders of magnitude. Dynamical cross-correlations between the component forces eliminate retardation of the total force.

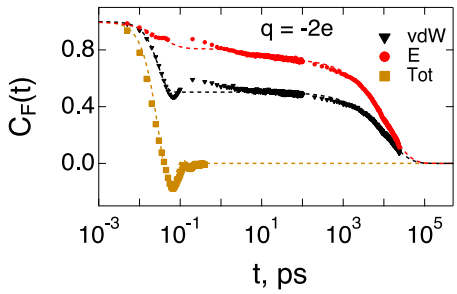

FIG. 15. Normalized force–force time correlation functions [Eq. (9)] for the vdW (black triangles), electrostatic (red circles), and total (mustard squares) forces acting from water on azurin carrying the total charge of $q = -2e$ (oxidized state). The dashed lines are fits to analytical functions. Reprinted with permission from S. M. Sarhangi and D. V. Matyushov, J. Phys. Chem. Lett. **11**, 10137 (2020). Copyright 2020 American Chemical Society.[45]

IV. DISCUSSION

Common to all diffusion phenomena is the gradient of osmotic pressure[3] allowing either a steady flux of solutes down the concentration gradient in Fickian diffusion or random force kicks in Brownian motion. When the tagged particle carries a charge or higher multipolar moments, mechanical equilibrium is established by density augmentation on the side of the particle where the liquid experiences a stronger electrostatic field [Eq. (1)]. The resulting enhancement of the vdW force either balances the electrostatic force completely or allows an uncompensated force in the body frame, which averages out to zero by particle rotations.

Mechanical equilibrium is established by balancing the vdW and electrostatic forces acting on a single molecule in the solvation layer. Even when the average total force in the body frame is nonzero [Fig. 11(b)], the average force $\tilde{f}$ acting on a molecule in the arrested solvation layer is close to zero. This requires $\delta\tilde{f}_E = -\delta\tilde{f}_{\rm vdW}$ for the fluctuations of single-particle forces [see Eqs. (35) and (38) for a full description of total forces]. This simple constraint makes thermal fluctuations of the component forces strongly correlate and leads to compensation relations in the force variance.

Reaching mechanical equilibrium in the solvation layer requires a sufficiently strong electrostatic pull from the solute charges close to the interface to allow the emergence of a structurally arrested solvation shell. The arrest applies only to the orientational manifold, still preserving the dynamical exchange of the solvent molecules between the solvation shell and the bulk. Compensation relations [Eqs. (26) and (27)] is a phenomenological signature of this new physical reality. It requires a new description of mobility, which, due to its specific physical nature, also allows some simplifications and general predictions. The destructive interference of the component forces shrinks the effective breadth of force fluctuations responsible for random kicks on a tagged particle. The arrested solvation layer is thus less noisy. The ensuring reduction of friction brings about higher diffusivity.

Tweaking the destructive interference between the component forces can potentially enhance diffusion.[104] Specifically, a chemical reaction instantaneously altering the solute charge distribution might induce a temporary shift of the balance between electrostatic and vdW forces and lead to a transient nonzero body-frame force $\langle\tilde{F}\rangle_t$ similar to the one observed for off-center solutes [Fig. 11(b)]. If the equilibration time for $\langle\tilde{F}\rangle_t \to 0$ is sufficiently long, one can potentially observe jerks in solute displacements analogous to enhanced mobility found for active matter.[105–107]

V. OUTLOOK

Moving forward, dielectric friction, while conceptually sound, turned out to be more complex phenomenologically than originally anticipated in Born's picture.[4] The effect of vdW-electrostatic cross correlations on the force variance is accounted for by the concept of arrested solvation layer and the balance between component forces

acting on the solute. The effect of cross correlations on the dynamics is much harder to describe theoretically. A significant speedup of the total force dynamics compared to the component forces is observed for both simple LJ ions [Fig. 1(b)] and proteins (Fig. 15). In the latter case, the speedup of the force dynamics by nearly six orders of magnitude presents a real challenge to theory. However, our understanding of dielectric friction is incomplete without a proper account for this phenomenology given that friction is overestimated by many orders of magnitude by traditional theories.

Translational diffusion turns out to be highly affected by the ionic charge for simple ions, but altering charge makes little effect on protein diffusion. The transition from high sensitivity of translational diffusion to the ionic charge for small ions to the lack of such sensitivity for colloidal particles, and the description of the intermediate length scale, will remain the subject for future studies. On a larger scale, establishing a clear link between statistical averages produced by atomistic simulations and standard parameters of continuous media used in colloidal science (slip plane, zeta potential, electromechanical forces, etc.) still remains an outstanding challenge for theory. The same note applies to nonlinear transport coefficients, such as dielectrophoresis.[108]

Much of the discussion here has focused on ionic and dipolar solutes in water since this is a much studied and practically important problem.[18–21] However, other polar solvents show similar phenomenology[57] and one anticipates that the general principles discussed here extend to other polar media.

ACKNOWLEDGMENTS

This research was supported by the National Science Foundation (Grant No. CHE-2154465).

AUTHOR DECLARATIONS

Conflict of Interest

The author has no conflicts to disclose.

Author Contributions

Dmitry V. Matyushov: Conceptualization (equal); Funding acquisition (equal); Writing – original draft (equal); Writing – review & editing (equal).

DATA AVAILABILITY

The data that support the findings of this study are available from the author upon request.

REFERENCES

[1]A. Einstein, *Investigations on the Theory of the Brownian Movement* (BN Publishing, 2011).
[2]J. K. G. Dhont, *An Introduction to Dynamics of Colloids*, Studies in Interface Science Vol. 2 (Elsevier Science, 1996).
[3]A. Einstein, *Z. Electrochem.* **14**, 235 (1908), in *Investigations on the Theory of the Brownian Movement*, edited by R. Furth (BN Publishing, 2011).
[4]M. Born, Z. Phys. **1**, 221 (1920).
[5]R. Kubo, *Lectures in Theoretical Physics* (Interscience Publishers, Inc., New York, 1959), Vol. 1, p. 120.
[6]R. Zwanzig, J. Chem. Phys. **38**, 1603 (1963).
[7]J. Hubbard and L. Onsager, J. Chem. Phys. **67**, 4850 (1977).
[8]P. G. Wolynes, Annu. Rev. Phys. Chem. **31**, 345 (1980).
[9]J. A. Stratton, *Electromagnetic Theory* (McGraw-Hill, New York, 1941).
[10]L. D. Landau and E. M. Lifshitz, *Electrodynamics of Continuous Media* (Pergamon, Oxford, 1984).
[11]J. R. Melcher, *Continuum Electromechanics* (MIT Press, Cambridge, MA, 1981).
[12]D. V. Matyushov, *Manual for Theoretical Chemistry* (World Scientific Publishing Co. Pte. Ltd., New Jersey, 2021).
[13]B. J. Berne and R. Pecora, *Dynamic Light Scattering* (Dover Publications, Inc., Mineola, NY, 2000).
[14]B. Bagchi, *Molecular Relaxation in Liquids* (Oxford University Press, Oxford, 2012).
[15]T. Kawasaki and K. Kim, Sci. Rep. **9**, 525 (2019).
[16]J. Wang, D. Bratko, and A. Luzar, J. Stat. Phys. **145**, 253 (2011).
[17]T. W. Nee and R. Zwanzig, J. Chem. Phys. **52**, 6353 (1970).
[18]M. Berkowitz and W. Wan, J. Chem. Phys. **86**, 376 (1987).
[19]S. Koneshan, J. C. Rasaiah, R. M. Lynden-Bell, and S. H. Lee, J. Phys. Chem. B **102**, 4193 (1998).
[20]S.-H. Chong and F. Hirata, J. Chem. Phys. **108**, 7339 (1998).
[21]J. C. Rasaiah and R. M. Lynden–Bell, Philos. Trans. R. Soc., A **359**, 1545 (2001).
[22]R. P. Feynman, R. B. Leighton, and M. Sands, *The Feynman Lectures on Physics*, Mainly Mechanics, Radiation, and Heat Vol. I (Addison-Wesley, Reading, MA, 1963).
[23]R. Kubo, Rep. Prog. Phys. **29**, 255 (1966).
[24]R. Zwanzig, Annu. Rev. Phys. Chem. **16**, 67 (1965).
[25]J.-P. Hansen and I. R. McDonald, *Theory of Simple Liquids*, 4th ed. (Academic Press, Amsterdam, 2013).
[26]U. Balucani and M. Zoppi, *Dynamics of the Liquid Phase* (Clarendon Press, Oxford, 1994).
[27]H. K. Shin, C. Kim, P. Talkner, and E. K. Lee, Chem. Phys. **375**, 316 (2010).
[28]R. Zwanzig, J. Chem. Phys. **52**, 3625 (1970).
[29]B. Bagchi and R. Biswas, Acc. Chem. Res. **31**, 181 (1998).
[30]X. Bian, C. Kim, and G. E. Karniadakis, Soft Matter **12**, 6331 (2016).
[31]G. van der Zwan and J. T. Hynes, J. Phys. Chem. **89**, 4181 (1985).
[32]D. V. Matyushov, J. Chem. Phys. **120**, 1375 (2004).
[33]T. Samanta and D. V. Matyushov, J. Chem. Phys. **153**, 044503 (2020).
[34]M. Maroncelli, J. Mol. Liq. **57**, 1 (1993).
[35]E. A. Carter and J. T. Hynes, J. Chem. Phys. **94**, 5961 (1991).
[36]H. Goldstein, *Classical Mechanics* (Addison-Wesley, Reading, MA, 1964).
[37]L. Onsager, J. Am. Chem. Soc. **58**, 1486 (1936).
[38]C. J. F. Böttcher, *Theory of Electric Polarization*, Dielectrics in Static Fields Vol. 1 (Elsevier, Amsterdam, 1973).
[39]J. B. Hubbard and P. G. Wolynes, J. Chem. Phys. **69**, 998 (1978).
[40]C. J. F. Böttcher, *Theory of Electric Polarization*, Deielctrics in Time-Dependent Fields Vol. 2 (Elsevier, 1973).
[41]B. K. P. Scaife, *Principles of Dielectrics* (Clarendon Press, Oxford, 1998).
[42]T. Samanta and D. V. Matyushov, J. Chem. Phys. **156**, 204501 (2022).
[43]G. Hummer, L. R. Pratt, A. E. García, B. J. Berne, and S. W. Rick, J. Phys. Chem. B **101**, 3017 (1997).
[44]T. Samanta and D. V. Matyushov, Phys. Rev. Res. **3**, 023025 (2021).
[45]S. M. Sarhangi and D. V. Matyushov, J. Phys. Chem. Lett. **11**, 10137 (2020).
[46]T. Samanta, S. M. Sarhangi, and D. V. Matyushov, J. Phys. Chem. Lett. **12**, 6648 (2021).
[47]A. Y. Cui and Q. Cui, J. Phys. Chem. B **125**, 4555 (2021).
[48]R. M. Lynden-Bell and J. C. Rasaiah, J. Chem. Phys. **107**, 1981 (1997).
[49]G. Hummer, L. R. Pratt, and A. E. García, J. Phys. Chem. A **102**, 7885 (1998).
[50]D. L. Mobley, A. E. Barber, C. J. Fennell, and K. A. Dill, J. Phys. Chem. B **112**, 2405 (2008).
[51]J. G. Davis, K. P. Gierszal, P. Wang, and D. Ben-Amotz, Nature **491**, 582 (2012).
[52]R. S. Hartman, D. S. Alavi, and D. H. Waldeck, J. Phys. Chem. **95**, 7872 (1991).
[53]M. L. Horng, J. A. Gardecki, A. Papazyan, and M. Maroncelli, J. Phys. Chem. **99**, 17311 (1995).

[54]E. W. Castner and M. Maroncelli, J. Mol. Liq. **77**, 1 (1998).
[55]G. B. Dutt, G. R. Krishna, and S. Raman, J. Chem. Phys. **115**, 4732 (2001).
[56]B. R. Gayathri, J. R. Mannekutla, and S. R. Inamdar, J. Fluoresc. **18**, 943 (2008).
[57]P. V. Kumar and M. Maroncelli, J. Chem. Phys. **112**, 5370 (2000).
[58]H. S. Frank and M. W. Evans, J. Chem. Phys. **13**, 507 (1945).
[59]S. Mondal and B. Bagchi, Nano Lett. **20**, 8959 (2020).
[60]D. B. Wong, K. P. Sokolowsky, M. I. El-Barghouthi, E. E. Fenn, C. H. Giammanco, A. L. Sturlaugson, and M. D. Fayer, J. Phys. Chem. B **116**, 5479 (2012).
[61]S. Perticaroli, L. Comez, P. Sassi, A. Morresi, D. Fioretto, and M. Paolantoni, J. Phys. Chem. Lett. **9**, 120 (2018).
[62]T. Fonseca and B. M. Ladanyi, J. Phys. Chem. **95**, 2116 (1991).
[63]P. K. Ghorai and D. V. Matyushov, J. Phys. Chem. B **110**, 1866 (2006).
[64]D. Bertolini, M. Cassettari, and G. Salvetti, J. Chem. Phys. **76**, 3285 (1982).
[65]T. Samanta and D. V. Matyushov, J. Mol. Liq. **364**, 119935 (2022).
[66]D. Laage and J. T. Hynes, Science **311**, 832 (2006).
[67]P. Madden and D. Kivelson, Adv. Chem. Phys. **56**, 467 (1984).
[68]S. Seyedi, D. R. Martin, and D. V. Matyushov, Phys. Rev. E **94**, 012616 (2016).
[69]R. Richert, Adv. Chem. Phys. **156**, 101 (2015).
[70]M. Saito, M. Kurokuzu, Y. Yoda, and M. Seto, Phys. Rev. E **105**, L012605 (2022).
[71]P. Debye, *Polar Molecules* (Dover Publications, New York, 1929).
[72]T. Keyes and D. Kivelson, J. Chem. Phys. **56**, 1057 (1972).
[73]D. Kivelson and P. Madden, Mol. Phys. **30**, 1749 (1975).
[74]A. Volmari and H. Weingärtner, J. Mol. Liq. **98-99**, 293 (2002).
[75]H. Weingärtner, H. Nadolny, A. Oleinikova, and R. Ludwig, J. Chem. Phys. **120**, 11692 (2004).
[76]D. Braun, S. Boresch, and O. Steinhauser, J. Chem. Phys. **140**, 064107 (2014).
[77]P. Honegger, M. Schmollngruber, and O. Steinhauser, Phys. Chem. Chem. Phys. **20**, 11454 (2018).
[78]G. Tarjus and D. Kivelson, J. Chem. Phys. **103**, 3071 (1995).
[79]M. D. Ediger, Annu. Rev. Phys. Chem. **51**, 99 (2000).
[80]X. Xia and P. G. Wolynes, J. Phys. Chem. B **105**, 6570 (2001).
[81]R. Richert, J. Phys.: Condens. Matter **14**, R703 (2002).
[82]M. G. Mazza, N. Giovambattista, H. E. Stanley, and F. W. Starr, Phys. Rev. E **76**, 031203 (2007).
[83]I. Chang and H. Sillescu, J. Phys. Chem. **101**, 8794 (1997).
[84]H. Sillescu, J. Non-Cryst. Solids **243**, 81 (1999).
[85]L. Berthier and G. Biroli, Rev. Mod. Phys. **83**, 587 (2011).
[86]J. D. Jackson, *Classical Electrodynamics* (Wiley, New York, 1999).
[87]D. J. Bonthuis, S. Gekle, and R. R. Netz, Phys. Rev. Lett. **107**, 166102 (2011).
[88]M. Dinpajooh and D. V. Matyushov, J. Chem. Phys. **145**, 014504 (2016).
[89]O. Teschke, G. Ceotto, and E. F. De Souza, Chem. Phys. Lett. **326**, 328 (2000).
[90]L. Fumagalli, A. Esfandiar, R. Fabregas, S. Hu, P. Ares, A. Janardanan, Q. Yang, B. Radha, T. Taniguchi, K. Watanabe, G. Gomila, K. S. Novoselov, and A. K. Geim, Science **360**, 1339 (2018).
[91]M. H. Motevaselian and N. R. Aluru, J. Phys. Chem. Lett. **11**, 10532 (2020).
[92]D. V. Matyushov, J. Phys. Chem. B **125**, 8282 (2021).
[93]M. Heyden and D. V. Matyushov, J. Phys. Chem. B **124**, 11634 (2020).
[94]D. R. Martin and D. V. Matyushov, J. Phys. Chem. Lett. **11**, 5932 (2020).
[95]E. H. Grant, R. J. Sheppard, and G. P. South, *Dielectric Behaviour of Biological Molecules in Solution* (Clarendon Press, Oxford, 1978).
[96]R. Pethig, Annu. Rev. Phys. Chem. **43**, 177 (1992).
[97]S. Takashima, J. Non-Cryst. Solids **305**, 303 (2002).
[98]S. D. Fried and S. G. Boxer, Acc. Chem. Res. **48**, 998 (2015).
[99]S. D. Fried and S. G. Boxer, Annu. Rev. Biochem. **86**, 387 (2017).
[100]M. E. Young, P. A. Carroad, and R. L. Bell, Biotech. Bioeng. **22**, 947 (1980).
[101]D. Brune and S. Kim, Proc. Natl. Acad. Sci. U. S. A. **90**, 3835 (1993).
[102]P. E. Smith and W. F. van Gunsteren, J. Mol. Biol. **236**, 629 (1994).
[103]M. Grimaldo, F. Roosen-Runge, F. Zhang, F. Schreiber, and T. Seydel, Q. Rev. Biophys. **52**, e7 (2019).
[104]A.-Y. Jee, Y.-K. Cho, S. Granick, and T. Tlusty, Proc. Natl. Acad. Sci. U. S. A. **115**, E10812 (2018).
[105]S. Ghosh, A. Somasundar, and A. Sen, Annu. Rev. Cond. Mat. Phys. **12**, 177 (2020).
[106]H. Wang, M. Park, R. Dong, J. Kim, Y.-K. Cho, T. Tlusty, and S. Granick, Science **369**, 537 (2020).
[107]Y. Zhang and H. Hess, Nat. Rev. Chem. **5**, 500 (2021).
[108]R. Pethig, *Dielectrophoresis. Theory, Methodology and Biological Applications* (Wiley, Hoboken, NJ, 2017).